
S.H. DHOBI,^{1,2,3} K. YADAV,^{1,3} S.P. GUPTA,^{1,3} J.J. NAKARMI,^{1,3} B. KOIRALA^{1,3}

¹ Innovative Ghar Nepal
(Lalitpur, Nepal)

² Robotics Academy of Nepal
(Lalitpur, Nepal)

³ Department of Physics, Patan Multiple Campus, Tribhuvan University
(Lalitpur, Nepal; e-mail: saddam@ran.edu.np)

DIFFERENTIAL CROSS-SECTION IN THE PRESENCE OF A WEAK LASER FIELD FOR INELASTIC SCATTERING

UDC 539

The objective of this work is to study the differential cross-section in the presence of a weak laser field (visible and UV) in the case of inelastic scattering. When the target absorbs the energy, the differential cross section increases, according to the theoretically constructed model. The differential cross-section initially decreases to a minimum and finally takes a maximum value, when the target emits the energy. The energy emission occurs at 5 eV, 10 eV, 13 eV, 16 eV, 20 eV, 25 eV, and 30 eV. In addition, the differential cross-section also increases with the scattering angle.

Keywords: inelastic scattering, laser field, scattering angle, differential cross-section.

1. Introduction

The experimental study of the scattering of electrons by atoms was executed by Franck and Hertz, and the early theoretical works were carried out by Massey and Mohr. During the last few decades, the study of electron-atom collisions in the presence of a laser field has been the subject of intense research activity. This is because of its importance in applied domains such as astrophysics, laser and plasma physics, and the fundamental atomic collision theory. Laser-assisted scattering is necessary, because, in the presence of laser-free electrons, it allows the absorption or emission of photons during the scattering processes by atoms. Due to advances in new experimental techniques, both elastic and inelastic electron-atom scatterings can be studied. Cionga *et al.* [1] calculated the differential cross-section for the elastic scattering in the presence of a laser for hy-

drogen atoms, using a static potential, the numerically obtained a differential cross-section of the order $(\log_{10} I^{-1} \frac{d\sigma}{d\Omega}) = 8$ maximum with high intensity $10^{12} \text{ W/cm}^{-2}$. Similarly, Bucia [12] calculated the differential cross-section in a similar way for the inelastic scattering of the same atom of the same order with high intensity $10^{10} \text{ W/cm}^{-2}$. But, at low intensities, no differential cross-section was studied for hydrogen atoms with polarized potential. This lack motivates the authors to calculate the differential cross-section.

Electron energy-loss spectroscopy is an analytical technique that measures changes in the kinetic energy of electrons after the interaction with the target. This technique allows one to study structural and chemical information about a solid on the atomic level. The energy resolution in this technique ranges from 1 eV to 0.1 eV. Moreover, the plasmon peaks, inner-shell ionization edges, as well as the fine structure, electronic densities of states, local properties, including the specimen thickness, mechanical and elec-

© S.H. DHOBI, K. YADAV, S.P. GUPTA, J.J. NAKARMI,
B. KOIRALA, 2022

ISSN 0372-400X. Укр. фіз. журн. 2022. Т. 67, № 4

227

tronic properties, and chemical composition, were discussed [3]. The Coulomb interaction between the incident electron and atomic electrons gives rise to the inelastic scattering within the interval of a few electron volts to hundreds of electron volts [4]. The target electron is a hydrogen atom electron, and its radius is about $\langle r^2 \rangle = 3a_0^2$, where a_0 is Bohr's radius and equal to $\frac{\hbar^2}{e^2 m_e}$. The dipole polarizabilities of this atom were calculated by different researchers and are limited by upper and lower bounds with

$$4a_0^3 \leq \alpha \leq \frac{16}{3} a_0^2$$

calculated by using the variational wave function approach. Some improvements were done by Dalfovo and Stringari with

$$\frac{33}{8} 4a_0^2 \leq \alpha \leq \frac{100}{21} a_0^2$$

and with the approximation method [4]. The range was set as

$$\frac{3}{4} 4a_0^2 \leq \alpha \leq 4.59 a_0^2,$$

which is well agreed with the upper bound.

The polarizability is defined as

$$\alpha^{nlm} = \alpha_0^{nl} + \alpha_2^{nl} \frac{3m^2 - l(l+1)}{l(2l-1)},$$

where α_0^{nl} and α_2^{nl} are known as the scalar and tensor polarizabilities. The polarizability depends upon three quantum numbers (n), azimuthal quantum number (l), and magnetic quantum number (m). The first term of the polarizability is scalar and depends on the principal quantum number and azimuthal quantum number, while the second term is a tensor and depends upon all three quantum numbers. For (n) = 1, (l) = 0, (m) = 0. Therefore, the polarizability only depends on the scalar term. More details can be found in [5], and the numerical values of the scalar and tensor polarizabilities are listed by Mitroy *et al.* in 2010. The electric (dipole) polarizability of a nucleus (or atom) is also defined by

$$\alpha_E = 2\alpha \sum_{N \neq 0} \frac{|\langle N | D_z | 0 \rangle|^2}{E_N - E_0}.$$

Moreover, we define, in terms of the cross-section,

$$\alpha_E = \frac{1}{2\pi} \int_{\omega_{th}}^{\infty} d\omega \frac{\sigma_{\gamma}^{ud}}{\omega^2}.$$

The significant sensitivity of α_E is also depends on the nuclear binding energies and was calculated using the no-core shell model (NCSM) in relative coordinates by Navratil *et al.* in 2007 and Hayes *et al.* in 2003 [6]. In a static homogeneous electric field, the dipole polarizability tensor of the ground electronic state is described by the quadratic Stark effect and is defined as

$$\alpha_{\alpha\beta} = 2 \sum_n \frac{\langle 0 | r_{\alpha} | n \rangle \langle n | r_{\beta} | 0 \rangle}{E_n - E_0}. \quad (1)$$

For the multielectron systems, the quadratic Stark shift is always negative for the ground state, whereas the dipole polarizability is always positive and non-zero (Saftonova *et al.*, 2015 and Delone *et al.*, 1999). The static scalar dipole polarizability for a neutral H-atom in 2s state is about 4.5 a.u. See more details in the works by Goldman, 1989; Tang *et al.*, 2012, and Filippin *et al.*, 2014. The isotopes of hydrogen ^1H and ^2H have approximate static polarizability with the fine structure constant. The directly measured value available for the hydrogen static dipole polarizability was measured by Scheffers and Stark as $\alpha = 4.0 \pm 1.3$ a.u. The dynamic dipole polarizability for hydrogen is 4.59 ± 0.07 a.u. (Scheffers, 1940). The experimental static dipole polarizability [7] for H_2 to be 5.437 a.u. yields a value equal to 4.503 ± 0.049 a.u. for atomic hydrogen (Marlow *et al.*, 1965 and Schuler *et al.*, 1925). Accurate theoretical estimates of the static and dynamic dipole polarizabilities are reported for the ground and excited states of hydrogen atoms. A variation of the computed polarizabilities is observed as a function of the number of grid points (Karplus *et al.*, 1972 and 1963). The dynamic polarizabilities of the 1s ground-state frequency interval $0 \leq \omega \leq 0.5$ a.u. at infinity (greater than 10 a.u.) is 4.5 a.u. reported in [8]. The infinite distance here is considered greater or equal to 20 a.u. The dynamic and static dipole polarizabilities are the same, i.e., 4.5 a.u. (Laughlin *et al.* 2002, Burrows *et al.*, 2005, and Montgomery, 2002).

The intensity of the laser field is as follows:

$$I = \frac{1}{2} \sqrt{\frac{\varepsilon_0}{\mu_0}} E_0^2 = \frac{\varepsilon_0 c E_0^2}{2}.$$

Here, ε_0 is the permittivity of the free space, μ_0 is the permeability, E_0 is the electric field, and c is the velocity of light. The behavior of an atom in high laser intensities $\geq 10^{13}$ W cm $^{-2}$ is usually analyzed basing on the Keldysh parameters given as

$$\gamma = \frac{\omega_0 \sqrt{2mI_0}}{eA},$$

here ω_0 is the frequency, m is the electron mass, I_0 is the ionization potential, A is the amplitude of the driver field, and e is the charge of the electron. In the present day, the laser intensities range from 10^{13} to 10^{17} W cm $^{-2}$ for a high-power laser with corresponding magnetic field strength 10^{10} to 10^{12} V/m. The recent development of the laser technology has resulted in the construction of short-pulse lasers capable of generating fs light pulses with PW powers and intensities exceeding 10^{21} W cm $^{-2}$, and has laid the basis for the multi-PW lasers, just being built in Europe [9]. This will produce fs pulses of ultra-relativistic intensities 10^{23} – 10^{24} W cm $^{-2}$. The intensity 6.53×10^{11} W/cm 2 , angular distribution (AD) has a bell shape with the maximum pointing perpendicularly to the laser polarization. Moreover, AD was computed for several laser field intensities in the range of 13×10^9 to 6.53×10^{11} W cm $^{-2}$ [10].

Laser-assisted electron scattering (LAES) involves the interaction between light and matter with the energy transfer between light fields and free electrons. Treiber *et al.* [11] studied the interaction of superfluid He in bulk between 32–340 Å with a strong laser field. Treiber *et al.* also reported that at high intensity the target from Xe and AC (acetone) gains an energy of 25–30 eV. LAES offers a unique advantage for time-resolved electron probes and can increase or decrease their kinetic energy by multiples of the photon energy $\pm n\hbar\omega$, in the presence of a strong laser field with atoms or molecules as the target. Kanya and Yamanouchi [12] showed that, above the threshold energy, the inelastic interactions are insignificant and have good agreement with a much lower cross-section as compared to the elastic interaction.

Double and triple differential cross-sections for the ionization of hydrogen-like atom was studied by Bidvari and Fathi [13] using the second Born approximation and showed that the ejected electron has energies of 16.4, 26.4, 36.4, and 39.4 eV, which is compared to both experimental and theoretical available results. The interaction of a laser field with un-

bound electrons (free electron) is treated in a non-perturbative way by the use of Volkov waves, which was proposed by Joachain *et al.* in 1988 for the electron ejected from the target with residual H $^+$ photon [14]. Ajana *et al.* [15] studied the differential cross-section for low energies using the Born approximation and obtained the total differential cross-section between 0 to 1.4 a.u. with the energy incidencing from 30 eV to 100 eV, and the laser photon energy was equal to 1.17 eV.

2. Material and Method

The polarized potential is given as

$$V(r) = -\frac{\alpha_p}{2(r^2 + d^2)^2}$$

and

$$d^2 = \frac{\alpha_p}{2Z^{1/3}},$$

where α_p is the dipole polarizability, and Z is the atomic number. The Fourier transformation for a polarized potential is

$$\tilde{V}(\Delta) = \frac{\alpha_p e^{-\Delta d}}{16\pi d}, \quad |\tilde{V}(\Delta)|^2 = \frac{\alpha_p^2 e^{-2\Delta d}}{256\pi^2 d^2}. \quad (2)$$

Using the Taylor series expansion and neglecting higher-order terms, we get

$$|\tilde{V}(\Delta)|^2 = \frac{\alpha_p^2}{256\pi^2 d^2}.$$

Then the scattering cross-section in terms of the transition matrix [16, 17] is given by

$$\frac{d\sigma}{d\Omega} = \frac{m^2}{(2\pi\hbar^2)^2} \frac{k_f}{k_i} |T_{k_f k_i}|^2, \quad (3)$$

$$|T_{k_f k_i}|^2 = \sum_l J_l^2(\Delta \cdot \alpha_0) |\tilde{V}(\Delta)|^2. \quad (4)$$

For $n = 1$, the Bessel function becomes

$$J_1(x) = \frac{(\Delta \cdot \alpha_0)^1}{2^1 \Gamma(1+1)} \times \left[1 - \frac{(\Delta \cdot \alpha_0)^2}{2 \cdot 2(1+1)} + \frac{(\Delta \cdot \alpha_0)^4}{2 \cdot 4 \cdot 2(1+1)(1+2)} + \dots \right]. \quad (5)$$

Here, dot (\cdot) indicates a dot product. If we consider ξ to be the angle between the electric field and the transform momentum, then

$$\Delta \cdot \alpha_0 = \Delta \alpha_0 \cos \xi. \quad (6)$$

For high frequencies and low intensities, the high order term in the Bessel function is neglected, because $\alpha_0 = \frac{eE_0}{m\omega^2}$. At the zero angle (momentum and electric field are parallel), the Bessel function is

$$J_1(\Delta.\alpha_0) = \frac{\Delta\alpha_0}{2},$$

and

$$[J_1(\Delta.\alpha_0)]^2 = \frac{\Delta^2\alpha_0^2}{4}.$$

For $n = -1$, we obtain

$$J_{-1}(\Delta.\alpha_0) = -\frac{\Delta\alpha_0}{2},$$

and

$$[J_{-1}(\Delta.\alpha_0)]^2 = \frac{\Delta^2\alpha_0^2}{4}.$$

Now, $|T_{k_f k_i}|^2$ becomes

$$|T_{k_f k_i}|^2 = \left(\frac{\alpha_0^2 \Delta^2 \alpha_p^2}{1024 \pi^2 d^2} \right). \quad (7)$$

Putting $\alpha_0 = \frac{eE_0}{m\omega^2}$, the differential cross-section follows from Eqs. (3) and (4) as

$$\frac{d\sigma}{d\Omega} = \frac{m^2}{(2\pi\hbar^2)^2} \frac{k_f}{k_i} \left(\frac{eE_0\Delta\alpha_p}{32md\pi\omega^2} \right)^2. \quad (8)$$

Since we consider the inelastic scattering, the change of the momentum $\Delta = k_f - k_i$, and the dot product of a change in the momentum gives

$$\Delta^2 = k_f^2 - 2k_f k_i \cos \theta + k_i^2. \quad (9)$$

Here, θ is the angle between k_f and k_i which is the scattering angle between the initial and final momenta of the projected particle (electron). Arranging Eq. (9) gives

$$\frac{\Delta^2}{k_i^2} = \frac{k_f^2}{k_i^2} - 2\frac{k_f}{k_i} \cos \theta + 1. \quad (10)$$

In the inelastic scattering, the energy is not conserved. Therefore, the energy of the final electron is equal to $E_{k_f} = E_{k_i} - l\hbar\omega \pm E_{oe}$. Here, E_{k_f} is the energy of the incidence electron, $\hbar\omega$ is the energy of a single photon in the laser field, E_{oe} is either the energy absorbed or emitted during the transformation (scattering). Moreover $+E_{oe}$ and $-E_{oe}$ denote, respectively, the energy gain and energy loss by the scattered electron as a result of the interaction of electrons and photons. Hence, this scattering is inelastic by definition. We have

$$\frac{E_{k_f}}{E_{k_i}} = \left(1 - \frac{l\hbar\omega}{E_{k_i}} \pm \frac{E_{oe}}{E_{k_i}} \right). \quad (11)$$

Here, E_{k_i} is the energy of the projected electron. In view of the relation $\frac{p^2}{2m}$, Eq. (11) gives

$$\frac{k_f}{k_i} = \left(1 - \frac{l\hbar\omega}{E_{k_i}} \pm \frac{E_{oe}}{E_{k_i}} \right)^{\frac{1}{2}}. \quad (12)$$

Substituting Eq. (10) in (12) and arranging, we get

$$\Delta^2 = k_i^2 \left(1 - \frac{l\hbar\omega}{E_{k_i}} \pm \frac{E_{oe}}{E_{k_i}} \right) - 2 \left(1 - \frac{l\hbar\omega}{E_{k_i}} \pm \frac{E_{oe}}{E_{k_i}} \right)^{\frac{1}{2}} \cos \theta + 1. \quad (13)$$

Now, we substitute Eq. (13) in the differential cross-section (8) and get

$$\begin{aligned} \frac{d\sigma}{d\Omega} &= \frac{m^2\alpha_0^2\alpha_p^2k_i^2}{4096\pi^4\hbar^4d^2} \left(1 - \frac{l\hbar\omega}{E_{k_i}} \pm \frac{E_{oe}}{E_{k_i}} \right)^{\frac{1}{2}} \times \\ &\times \left[\left(1 - \frac{l\hbar\omega}{E_{k_i}} \pm \frac{E_{oe}}{E_{k_i}} \right) - 2 \left(1 - \frac{l\hbar\omega}{E_{k_i}} \pm \frac{E_{oe}}{E_{k_i}} \right)^{\frac{1}{2}} \cos \theta + 1 \right]. \end{aligned} \quad (14)$$

Multiplying Eq. (14) by \hbar^2 with $\alpha_0 = \frac{eE_0}{m\omega^2}$ and solving the resulting equation, we get

$$\begin{aligned} \frac{d\sigma}{d\Omega} &= \frac{m^2\alpha_0^2\alpha_p^2E_0^2E_{k_i}^2\lambda^4}{32378\pi^4\hbar^4d^2c^2} \left(1 - \frac{l\hbar\omega}{E_{k_i}} \pm \frac{E_{oe}}{E_{k_i}} \right)^{\frac{1}{2}} \times \\ &\times \left[\left(1 - \frac{l\hbar\omega}{E_{k_i}} \pm \frac{E_{oe}}{E_{k_i}} \right) - 2 \left(1 - \frac{l\hbar\omega}{E_{k_i}} \pm \frac{E_{oe}}{E_{k_i}} \right)^{\frac{1}{2}} \cos \theta + 1 \right]. \end{aligned} \quad (15)$$

Let

$$C = \frac{me^2\alpha_p^2}{3237\pi^8\hbar^6d^2c^4} = 1.65 \times 10^{-10},$$

where $\alpha_p = 4.5$ a.u. is the dipole at a distance greater than 10 a.u. Hence, we can consider that $d = 20$ a.u. and

$$\begin{aligned} \frac{d\sigma}{d\Omega} &= \frac{CE_0^2E_{k_i}^2}{\omega^4} \left(1 - \frac{l\hbar\omega}{E_{k_i}} \pm \frac{E_{oe}}{E_{k_i}} \right)^{\frac{1}{2}} \times \\ &\times \left[\left(1 - \frac{l\hbar\omega}{E_{k_i}} \pm \frac{E_{oe}}{E_{k_i}} \right) - 2 \left(1 - \frac{l\hbar\omega}{E_{k_i}} \pm \frac{E_{oe}}{E_{k_i}} \right)^{\frac{1}{2}} \cos \theta + 1 \right]. \end{aligned} \quad (16)$$

Here, $\omega = 2\pi f = 2\pi\frac{c}{\lambda}$ is the number of photons transferred during the interaction. Now, in the

atomic units, the inelastic differential cross-section from Eq. (16) becomes

$$\frac{d\sigma}{d\Omega} = \frac{CE_0^2 E_{k_i}^2}{\omega^4} \left[\left(1 - \frac{l\hbar\omega}{E_{k_i}} \pm \frac{E_{oe}}{E_{k_i}}\right)^{\frac{3}{2}} - 2 \left(1 - \frac{l\hbar\omega}{E_{k_i}} \pm \frac{E_{oe}}{E_{k_i}}\right) \cos\theta + \left(1 - \frac{l\hbar\omega}{E_{k_i}} \pm \frac{E_{oe}}{E_{k_i}}\right)^{\frac{1}{2}} \right]. \quad (17)$$

Assuming $x = \frac{l\omega}{E_{k_i}} \pm \frac{E_{oe}}{E_{k_i}}$ in Eq. (17) and using the expansions for the first and third terms, we get

$$\begin{aligned} \left(1 - \frac{l\hbar\omega}{E_{k_i}} \pm \frac{E_{oe}}{E_{k_i}}\right)^{\frac{3}{2}} &= \\ &= (1-x)^{\frac{3}{2}} = 1 - \frac{3}{2}x - \frac{3}{4}\frac{x^2}{2!} + \frac{3}{8}\frac{x^3}{3!} - \dots \end{aligned} \quad (18)$$

Taking the first two terms for a better solution, we have

$$\left(1 - \frac{l\hbar\omega}{E_{k_i}} \pm \frac{E_{oe}}{E_{k_i}}\right)^{\frac{3}{2}} = (1-x)^{\frac{3}{2}} = 1 - \frac{3}{2} \left(\frac{l\omega}{E_{k_i}} \pm \frac{E_{oe}}{E_{k_i}}\right). \quad (19)$$

Similarly, for the third term, we get

$$\left(1 - \frac{l\hbar\omega}{E_{k_i}} \pm \frac{E_{oe}}{E_{k_i}}\right)^{\frac{1}{2}} = (1-x)^{\frac{1}{2}} = 1 - \frac{1}{2} \left(\frac{l\omega}{E_{k_i}} \pm \frac{E_{oe}}{E_{k_i}}\right). \quad (20)$$

Now, from Eqs. (17), (19), and (20), we obtain

$$\frac{d\sigma}{d\Omega} = \frac{4CE_0^2 E_{k_i}^2}{\omega^4} \left(1 - \frac{l\omega}{E_{k_i}} \pm \frac{E_{oe}}{E_{k_i}}\right) \sin^2 \frac{\theta}{2}. \quad (21)$$

Here, E_{oe} is the energy which is either gained by the electron or lost by the incidence electron after the scattering. This equation represents the differential cross-section for the inelastic scattering. Moreover, this equation indicates a different condition.

Case I: The energies of the incidence electron and photo (laser field) are not greater than the threshold energy of atom's electron. Then Eq. (21) becomes

$$\left(\frac{d\sigma}{d\Omega}\right)_{E_{k_i}, E_p < E_{th}} = \frac{4CE_0^2 E_{k_i}^2}{\omega^4} \left(1 \pm \frac{E_{oe}}{E_{k_i}}\right) \sin^2 \frac{\theta}{2}. \quad (22)$$

This is true, because the $l\omega$ term doesn't play any role in the interaction, although the scattering takes place in the presence of a laser field or photons.

Case II: The energies of the incidence electron and photon (laser field) are greater than the threshold of

atom's electron. Then Eq. (21) is a fit for this condition. We have

$$\left(\frac{d\sigma}{d\Omega}\right)_{E_{k_i}, E_p > E_{th}} = \frac{4CE_0^2 E_{k_i}^2}{\omega^4} \left(1 - \frac{l\omega}{E_{k_i}} \pm \frac{E_{oe}}{E_{k_i}}\right) \sin^2 \frac{\theta}{2}. \quad (23)$$

Comparison of the differential cross-section:

$$\frac{\left(\frac{d\sigma}{d\Omega}\right)_{E_{k_i}, E_p < E_{th}}}{\left(\frac{d\sigma}{d\Omega}\right)_{E_{k_i}, E_p > E_{th}}} = \frac{\left(1 \pm \frac{E_{oe}}{E_{k_i}}\right)}{\left(1 - \frac{l\omega}{E_{k_i}} \pm \frac{E_{oe}}{E_{k_i}}\right)}. \quad (24)$$

The relation

$$\left(1 \pm \frac{E_{oe}}{E_{k_i}}\right) > \left(1 - \frac{l\omega}{E_{k_i}} \pm \frac{E_{oe}}{E_{k_i}}\right)$$

holds, because the two-term expression is the same in both cases, and $\frac{l\omega}{E_{k_i}}$ in $\left(1 - \frac{l\omega}{E_{k_i}} \pm \frac{E_{oe}}{E_{k_i}}\right)$ is the additional negative term. Therefore, we have

$$\frac{\left(\frac{d\sigma}{d\Omega}\right)_{E_{k_i}, E_p < E_{th}}}{\left(\frac{d\sigma}{d\Omega}\right)_{E_{k_i}, E_p > E_{th}}} = \frac{\left(1 \pm \frac{E_{oe}}{E_{k_i}}\right)}{\left(1 - \frac{l\omega}{E_{k_i}} \pm \frac{E_{oe}}{E_{k_i}}\right)} > 1, \quad (25)$$

$$\left(\frac{d\sigma}{d\Omega}\right)_{E_{k_i}, E_p < E_{th}} > \left(\frac{d\sigma}{d\Omega}\right)_{E_{k_i}, E_p > E_{th}}. \quad (26)$$

This equation shows that the differential cross-section of the scattering with the incidence energies of an electron and a photon less than the threshold (E_{th}) is greater than the differential cross-section of the scattering with incidence energies of an electron and a photon greater than the threshold. The differential cross-section is greater, since the electron-target interaction during the collision forces electrons to oscillate. The target electrons do not escape the orbits of the atom due to the insufficient incidence in the energy of the electron. But the differential cross-section decreases. When the energies of a photon and the incidence electron are high, the electrons have no time to oscillate. Moreover, the electron goes to an excited state after the energy absorption from the laser field (photon).

3. Results and Discussion

The energy ranges for the differential cross-section for the scattering of electrons by helium were studied in the interval 1–20 eV with a high-intensity carbon dioxide laser. The reported cross-sections are

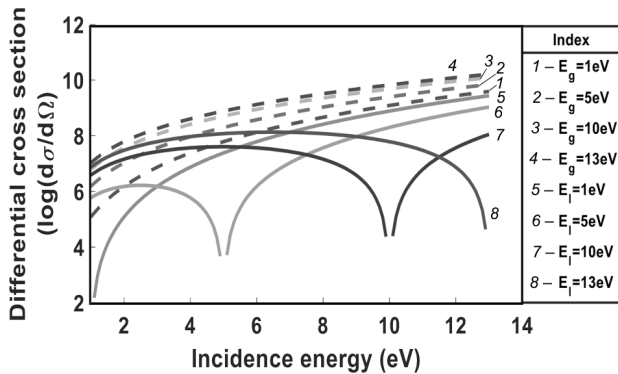


Fig. 1. Differential cross-section area with the incidence energy of the electron during the inelastic collision at $\theta = 10^\circ$ and $\omega = 0.5$ a.u.

not zero, but confirm similar experiments with argon as the scattering centers reported in [18]. Therefore, the authors are using visible and UV ranges of the electron energy for hydrogen atoms, because there are no studies of the scattering in such energy interval. Some authors studied the differential cross-section with high-energy electrons from a few keV to MeV like Joachain [19], Buica [2], etc. To study the differential cross-section, one can use Nd:YAG ($\omega = 1.17$ eV) or He:Ne ($\omega = 2$ eV) lasers in earlier laser-assisted electron-atom experiments used by Hark *et al.* in 2011 and other researchers.

3.1. Inelastic differential cross-section in a weak laser field with the energies of incidence electron and the photon less than the threshold

In the inelastic scattering, the electron absorbs or emits the energy during the interaction. Therefore, the energies after and before the reaction or interaction are not equal. Equation (22) developed above shows the differential cross-section for the inelastic scattering. The dashed curve (line) in Fig. 1 shows the differential cross-section when gaining the energy during a collision. This means that the final energy of the electron after the scattering is greater than the initial one. But the undashed and smooth curves show electrons which lose the energy after the scattering. The graph below also shows that the differential cross-section is greater, when electrons gain energy, while it is less, when electrons lose the energy during the scattering. Moreover, when electrons lose the 1-eV energy, the nature of differential cross-section is

the same as the electron gain energy. But when electrons absorb 5 eV and 10 eV, the nature of differential cross-section is different. It decreases initially and then increases. In the figures E_l represent the energy loss from the target to the field and electron, whereas E_g represents the energy gain from the field and electron by the target.

The differential cross-section increases with the energy of the incidence electron, when the electron loses the energy of 1 eV during the inelastic scattering. This occurs, because the energy loss is very low and causes the electron oscillation. But as the energy loss of the incidence electron after the scattering (between 5 eV and 10 eV), the differential cross-section decreases, as the incidence energy of the electron increases. At the interaction point, the energy transfer occurs, and the breaking point is observed. Note that the oscillations cause an increase in the differential cross-section. The decreased cross-section means that the energy of the incidence electron transforming to a target electron and at a low differential cross-section, the maximum energy transformation takes place, due to which the target electron oscillation happens. Hence, the differential cross-section increases and becomes maximum at a resonance state. Therefore, the differential cross-section firstly decreases and then increases after the transformation of the energy at breakpoints (5 eV and 10 eV) with the energy loss. When electrons lose the 13-eV energy to the target, the differential cross-section decreases and becomes low, because the electron goes to an excited or Fermi state.

3.2. Inelastic differential cross section in a weak laser field with scattering angle

The differential cross-section with some scattering angle and at the 10-eV incidence electron energy is shown in Fig. 2. The differential cross-section increase with the scattering angle, but the differential cross-section during the energy gain is greater than at he energy loss. Such pattern is seen, because the target electron gains energy from the incidence electron and oscillates, due to which the cross-sections in both cases increase. When the electron gain energy oscillation enhances, the differential cross-section is higher than in the energy loose cases.

3.3. Inelastic differential cross section in a weak laser field when the energies of the incidence electron and a photon are greater than the threshold

Figure 3 shows the differential cross-section of the inelastic scattering with $l = 1$ (emission of one photon). When the scattering takes place in a laser field (photon energy is greater than the threshold of the target electron atom), and the emission of a photon occurs. The emission of a photon takes place, when the incidence electron transfers a partial energy to the target electron which absorbs the energy from photons and goes to an excited state. By emitting photons, it transits to the ground state. In this way, the photon is emitted ($l = 1$), and the scattered electron either absorbs or loses the energy at that instant. The dashed curve shows the energy gained by the electron during the target-electron interaction. But the smooth curve shows that scattered electrons lose energy during the interaction of the target, incidence electron, and photons at an instant. The breakpoint in the figure is due to the transformation of the energy between the electrons after the oscillation which increases and decreases the differential cross area. The decrease in the differential cross-section happens due to the transformation of the energy to the target. After the interaction, the differential cross-section increases due to the oscillation of electrons.

Figure 4 represents a differential cross-section of the inelastic scattering with $l = -1$ (absorption of one photon). When the scattering takes place in the laser field (photon energy is greater than the threshold of the target electron atom), and the absorption of one photon is realized, the absorption of a photon occurs, when the incidence electron transforms a partial energy to the target electron, and the target electron absorbs the energy from the photon instantly (laser field). The dashed curve shows that the energy is gained by the scattered electrons during the interaction. The smooth curve shows that scattered electrons lose energy.

The numerically calculated differential cross-section is obtained for the ranges such as $\log(\frac{d\sigma}{\Omega}) = 2$ to $\log(\frac{d\sigma}{\Omega}) = 12$. This is comparable with the differential cross-section obtained by Burica for the inelastic scattering and Cionga *et al.* for the elastic differential cross-section for a hydrogen atom. As Kanya and Yamanouchi [12] reported, the differential cross-section above the threshold energy for inelastic in-

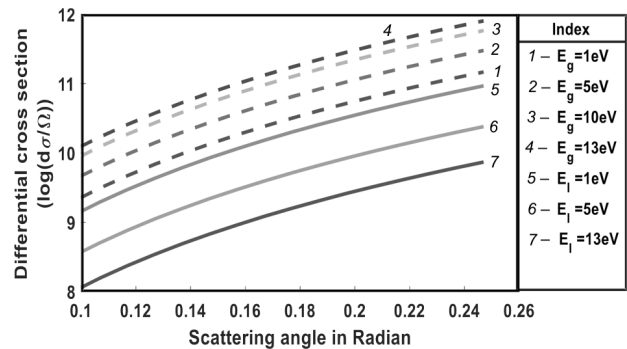


Fig. 2. Differential cross-section at a scattering angle in the inelastic scattering

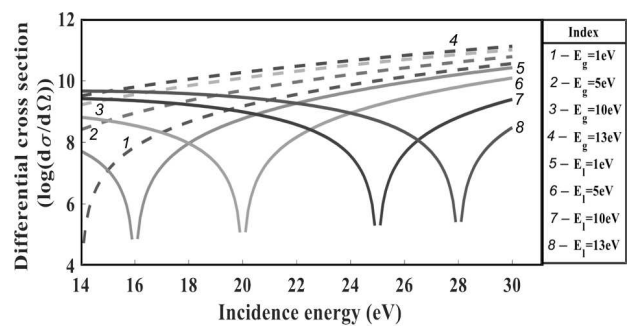


Fig. 3. Differential cross-section with $l = 1$ and the energy greater than the threshold

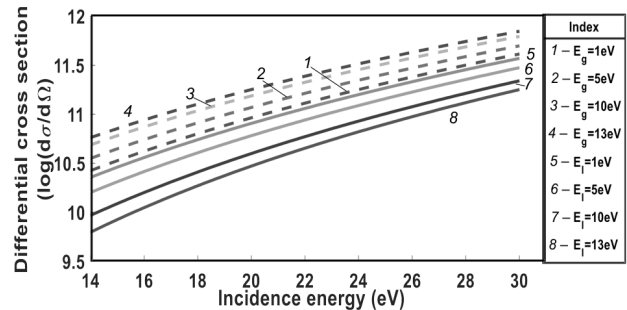


Fig. 4. Differential cross-section during the absorption of a photon

teractions is very lower in comparison to the elastic interaction. Therefore, the calculated differential cross-section by the authors in this work ranges from 1.5 a.u. to 12 a.u. which is also small and agrees with Kanya and Yamanouchi. In addition, the differential cross-section calculated by Ajana *et al.* [15] ranges from 0 to 1.4 a.u. for low energies (30 eV to 100 eV) with a laser photon energy of 1.17 eV. The maximum differential cross-section was calculated by Ajana *et al.*, and the minimum found by the authors

is 0.1 a.u. Since the authors consider low incidence energies (1 eV to 30 eV), the differential cross-section is dependent upon $\left(1 \pm \frac{\hbar\omega}{E_{k_i}}\right)$. For the lower value of the incidence energy, a higher differential cross-section was observed to be hence greater than that given by Ajana et al.

4. Conclusion

The developed mathematical equations (21) and (22) are used to study the differential cross-sections in the presence of a weak laser field for the inelastic scattering. Equation (21) is visualized in Figs. 3 and 4 based on a laser field intensity of 10^6 W/cm⁻² and the incidence energy greater than the ground-state energy of a hydrogen atom. Similarly, Eq. (22) is visualized in Figs. 1 and 2 based on the same intensity and incidence energy less than the ground-state energy of the hydrogen atom. The differential cross-section was found greater, when scattered electrons gain energy instead of its loss from the system. The differential cross-section was found minimum at 5, 10, 13, 16, 20, 25, and 30 eV, because the target emits the energy to the system. In addition, the differential cross-section increases with the scattering angle.

The authors would like to thank all members of the innovative Ghar Nepal, robotics academy of Nepal, Department of Physics, Patan Multiple campus for providing the peaceful environment during the work.

1. A. Cionga, F. Ehlötzky, G. Zloh. Elastic electron scattering by excited hydrogen atoms in a laser field. *Phys. Rev. A* **64**, 043401 (2001).
2. G. Buica. Inelastic scattering of electrons by metastable hydrogen atoms in a laser field. *Phys. Rev. A* **92**, 033421 (2015).
3. R.F. Egerton. Electron energy-loss spectroscopy in the TEM. *Rep. Prog. Phys.* **72**, (2009).
4. M. Traini. Electric polarizability of hydrogen atom: a sum rule approach. *Eur. J. Phys.* **17**, (1996).
5. D. Baye. Exact nonrelativistic polarizabilities of the hydrogen atom with the Lagrange-mesh method (2012) [DOI: <https://core.ac.uk/download/pdf/193934201.pdf>].
6. I. Stetcu, S. Quaglioni, J.L. Friar, A.C. Hayes, P. Navratil. Electric dipole polarizabilities of hydrogen and helium isotopes. arxiv.org/pdf/0904.3732.pdf.
7. P. Schwerdtfeger, J.K. Nagle. 2018 Table of static dipole polarizabilities of the neutral elements in the periodic table. *Mol. Phys.* **117**, 9 (2019).
8. S. Cohen, S.I. Themelis, K.D. Sen. dynamic dipole polarizabilities of the ground and excited states of confined hydrogen atom computed by means of a mapped fourier Grid method. *Int. J. Quantum Chem.* **108**, 351 (2008).

9. J. Badziak. Laser-driven ion acceleration: methods, challenges and prospects, International Conferences on Research and Applications of Plasmas. *IOP Conf. Series: J. Phys.: Conf. Series* **959**, 012001 (2018).
10. D.A. Telnov, S.I. Chu. Angular distributions from two-photon detachment of HÁ near ionization threshold: Laser-frequency and -intensity effects. *Phys. Rev. A* **66**, 063409 (2002).
11. L. Treiber, B. Thaler, P. Heim, M. Stadlhofer, R. Kanya, M.K. Zeiler, M. Koch. Observation of laser-assisted electron scattering in superfluid helium. *Nat. Commun.* **12**, 4204 (2021).
12. R. Kanya, K. Yamanouchi. Femtosecond laser-assisted electron scattering for ultrafast dynamics of atoms and molecules. *Atoms* **7**, 85 (2019).
13. S.A. Bidvari, R. Fathi. Triple and double differential cross sections for ionization of atomic hydrogen by positive-bare ions impact. *Eur. Phys. J. D* **74**, 55 (2020).
14. I. Ajana, A. Makhoute, D. Khalil, A. Dubois. The second Born approximation in laser assisted (e, 2e) collisions in hydrogen. *J. Phys. B: At. Mol. Opt. Phys.* **47**, 175001 (2014).
15. B.A. Harak, B.N. Kim, C.M. Weaver, N.L.S. Martin, M. Siavashpouri, B. Nosarzewski. Effects of polarization direction on laser-assisted free-free scattering. *Plasma Sources Sci. Technol.* **25**, 035021 (2016).
16. K. Yadav, J.J. Nakarmi. The elastic scattering of an electron from the target by absorbing a photon via free-free scattering theory. *Int. J. Mech. Eng. And Appl.* **2**, 6 (2014).
17. K. Yadav, J.J. Nakarmi. Elastic scattering of an electron via free-free scattering theory. *Condens. Matter Phys.* **81** (2015).
18. B. Wallbank, J.K. Holmes. Laser-assisted elastic electron scattering from helium. *Can. J. Phys.* **79**, 10 (2001).
19. C.J. Joachain. Laser-assisted electron-atom collisions. *Laser Chem.* **11**, 273 (1991).

Received 18.04.21

С.Х. Дхобі, К. Ядав,

С.П. Гупта, Дюс.Дюс. Накармі, В. Койрала

ДИФЕРЕНЦІАЛЬНИЙ ПЕРЕРІЗ ДЛЯ НЕПРУЖНОГО РОЗСІЮВАННЯ У ПРИСУТНОСТІ СЛАБКОГО ПОЛЯ ЛАЗЕРА

Ми вивчаємо диференціальний переріз непружного розсіювання у присутності слабкого поля лазера (видиме світло та ультрафіолет). Коли мішень поглинає енергію, диференціальний переріз зростає згідно з теоретичною моделлю. Диференціальний переріз спочатку зменшується до мінімуму та потім досягає максимального значення, коли мішень випромінює енергію. Випромінювання енергії відбувається при 5, 10, 13, 16, 20, 25 і 30 еВ. Крім того, диференціальний переріз зростає зі збільшенням кута розсіювання.

Ключові слова: непружне розсіювання, поле лазера, кут розсіювання, диференціальний переріз.